# Determination of the Difference Potential from Resonant Charge-Exchange Total Cross Sections: Analysis of $Rb^+$-Rb and $Cs^+$-Cs

R. E. Olson*
*Stanford Research Institute, Menlo Park, California* 94025
(Received 21 April 1969)

Within a two-state formalism, a systematic procedure is developed for deriving the difference between the *gerade* and *ungerade* state potentials from resonant charge-exchange total cross sections. It is shown that three potential constants may be derived from (i) the relative monotonic velocity dependence of the cross sections, (ii) the absolute scaling factor, and (iii) the frequency of the interference oscillations. The method is applied to the $Rb^+$-Rb and $Cs^+$-Cs experimental cross-section measurements of Perel, Vernon, and Daley. The difference potential for $Rb^+$-Rb is found to exhibit a maximum at 5.6 a.u. with a magnitude of 3.0 eV. The $Cs^+$-Cs data are likewise analyzed and a maximum of 2.3 eV is located at 6.5 a.u. In both cases, the error estimates are about ±25%.

## INTRODUCTION

Within the boundaries of the validity of the two-state approximation and in the low-keV energy region, it is well established that the difference potential between the *gerade* and *ungerade* ground states of a symmetric system controls the resonant charge-exchange total cross sections.[1] Experimental measurements, such as those by Perel, Vernon, and Daley on the Rb and Cs systems,[2] may hence be used to deduce information about this difference potential.

In the above experimental observations, the cross sections were found to obey the general relationship $Q^{1/2} = a - b \ln v$. The most interesting aspect, however, was an oscillatory structure that was seen superimposed upon this monotonic velocity dependence. This oscillatory structure may be interpreted by a two-state stationary phase argument[3] that predicts its occurrence whenever the difference potential between the *gerade* and *ungerade* states exhibits a maximum. This same concept has been used to predict that oscillations would also appear in the cross sections of the $Li^+$-Li system.[4]

The object of this work is to provide a convenient method for analyzing the resonant charge-exchange cross sections. A systematic procedure is set up for determining three parameters of the difference potential from (i) the relative monotonic velocity dependence of the cross sections, (ii) the absolute scaling factor, and (iii) the frequency of the interference oscillations. A hypothetical test case is examined and explained. Then, using the methods described within, the $Rb^+$-Rb and $Cs^+$-Cs experimental cross sections[2] are analyzed. A check is also made by retrieving the difference potential from $Li^+$-Li theoretical cross sections[4] which were calculated by an independent method.

## THEORY

In the two-state region of validity, the resonant charge-exchange total cross section is given by[1]

$$Q_{01} = (\pi/k^2)\sum (2l+1)\sin^2(\eta_l^+ - \eta_l^-)\,. \qquad (1)$$

Here $k$ is the wave number of the colliding system, we have $k = \mu v/\hbar$ as usual, and $\eta_l^{\pm}$ are the phase shifts for the *gerade* and *ungerade* states. Except at small impact parameters $b$ and at low velocities, the difference in phase shifts may be approximated by[1]

$$\Delta\eta(b) = \eta^+(b) - \eta^-(b) = -\frac{1}{\hbar v}\int_b^\infty \frac{r[V^+(r) - V^-(r)]\,dr}{(r^2 - b^2)^{1/2}}\,, \qquad (2)$$

where the semiclassical relation $b = (l + \frac{1}{2})/k$ has been utilized.

If the difference potential $V^+(r) - V^-(r)$ possesses a maximum or a minimum, interference effects will arise from collisions at large impact parameters, and from collisions at a much smaller impact parameter corresponding to the stationary point. A stationary point occurs specifically whenever $\Delta\eta(b)$ possesses a maximum or a minimum. It is defined as the impact parameter for which $d\Delta\eta(b)/db$ is equal to zero. This interference between collisions from the two impact parameters will produce an oscillatory structure in the cross sections. The stationary-phase approximation[5] may be employed to determine Eq. (1), yielding[3]

$$Q_{01} = \bar{Q} - (\pi^{3/2} b_0)\left(\left|\frac{d^2\Delta\eta(b)}{db^2}\right|\right)_{b=b_0}^{-1/2} \times \cos[2\Delta\eta(b_0) + \gamma]\,, \qquad (3)$$

where $b_0$ is the impact parameter at the stationary point. $\bar{Q}$ is the monotonic portion of the cross

section, which may be represented by

$$\bar{Q} = \tfrac{1}{2}\pi b_F^{\,2}, \tag{4}$$

in which $b_F$ is the Firsov impact parameter,[6] for which $|\Delta\eta(b_F)| = 1/\pi$. (The use of this relationship has been confirmed by the author to yield $\bar{Q}$ within ±5% of computed cross sections for a variety of exponential difference potentials.) The quantity $\gamma$ of Eq. (3) is equal to $-\frac{1}{4}\pi$ for a difference potential that has a minimum, and is equal to $+\frac{1}{4}\pi$ for a difference potential with a maximum.

If a given system possesses a stationary point, we see from Eq. (2) that

$$\Delta\eta(b_0) = \text{const} \times v^{-1} \ . \tag{5}$$

Hence in Eq. (3), the amplitude of the oscillations will be proportional to $v^{1/2}$, and the frequency will be proportional to $v^{-1}$. This is a general relationship which is not dependent upon the functional forms of $V^+(r)$ and $V^-(r)$.

Recalling the studies on the glory oscillations in atom-atom scattering,[7] one obtains a similar condition for the cross section extrema in the present case, except that now reference will be made to the difference potential and the difference in phase shifts as compared to the one-channel elastic case. As the velocity is varied, extrema will occur when the difference in the phase shifts at the stationary-point impact parameter proceeds through multiples of $\frac{1}{2}\pi$. Specifically, the extrema of the cross sections and difference phase shifts may be parametrized as

$$\Delta\eta(b_0) = \pm(N - \tfrac{3}{8})\pi \ , \tag{6}$$

where $N = 1, 2, 3, \ldots$ are indices for the maxima, and $N = 1.5, 2.5, 3.5, \ldots$ refer to the minima. [The plus or minus sign of Eq. (6) refers to difference potentials that have a minimum or a maximum, respectively.] If the cross sections are plotted versus $v^{-1}$ and sequenced in the order above, a plot of $N$ versus $v^{-1}$ will have an intercept of $\frac{3}{8}$, and the slope will determine the constant of Eq. (5) which is composed of all the potential parameters. An example will follow in the next section.

## TEST CASE

In the test case, functional forms for the potentials of both states should be employed that are physically reasonable and, for continuity with the analysis, that also have enough flexibility to fit the experimental data. Another requirement is that the number of parameters be kept within the informational content of the experimental measurements. For these reasons both a Morse and an exponential potential of the following functional forms are utilized[8]:

$$V^-(r) = D_e[e^{2\alpha(1-r/r_e)} - 2e^{\alpha(1-r/r_e)}] \ ,$$
$$V^+(r) = 2D_e e^{\alpha(1-r/r_e)} \ . \tag{7}$$

The repulsive potential $V^+(r)$ is determined by the parameters of $V^-(r)$. The symmetrical separation at large internuclear separations satisfies first-order perturbation theory. This criterion will not be true at small separations. However, the observable quantity is the difference potential, and Eqs. (7) are used to justify the plausibility of utilizing a functional form for the difference potential of $a_1 e^{-2a_2 r} - a_3 e^{-a_2 r}$. Combining Eqs. (7), we obtain for the difference potential

$$V^+(r) - V^-(r) = 4D_e e^{\alpha(1-r/r_e)} - D_e e^{2\alpha(1-r/r_e)} \ . \tag{8}$$

The parameters $D_e$, $\alpha$, and $r_e$ are retained so that crude estimates can be made about the separated potentials. The maximum of the difference potential will occur at $r = R_{\max}$ defined by $\exp(-\alpha R_{\max}/r_e) = 2/\exp(\alpha)$, with a value $\Delta V_{\max} = 4D_e$.

A test case was used in order to check the predictions of the stationary-phase approximation. Eq. (3). Here, the phase shifts were computed via Eq. (2), and the resonant charge-exchange total cross sections were calculated by the use of Eq. (1) (the stationary-phase approximation was *not* utilized in the computations). The input parameters were $r_e = 5.0$ a.u., $\alpha = 2.5$, $D_e = 0.25$ eV, and the reduced mass $\mu = 843$ a.u. A velocity region was scanned, and the results are presented in Fig. 1.

In the high-velocity limit, however, Eq. (2) may be solved in closed form for a difference potential such as Eq. (8). The solution is in terms of modified Bessel functions of the second kind.[9] Redefining Eq. (8) by letting $A = 4D_e e^{\alpha}$ and $B = \alpha/r_e$, we may rewrite the difference potential as

$$V^+(r) - V^-(r) = Ae^{-Br}(1.0 - \tfrac{1}{4}e^{\alpha}e^{-Br}) \ . \tag{9}$$

Allowing $\beta = B \cdot b$, we obtain for Eq. (2)

$$\Delta\eta(\beta) = -(A/B\hbar v)[\beta K_1(\beta) - \tfrac{1}{8}e^{\alpha} 2\beta K_1(2\beta)] \ . \tag{10}$$

Remembering that the monotonic portion of the cross sections can be interpreted in terms of the Firsov impact parameter, we may define a reduced cross section as

$$\bar{Q}_*^{1/2} = (\tfrac{1}{2}\pi)^{1/2}\beta_F = (\tfrac{1}{2}\pi)^{1/2} B b_F \ , \tag{11}$$

with the relationship to $\bar{Q}$ being

$$\bar{Q}^{1/2} = \bar{Q}_*^{1/2} B^{-1} \ . \tag{12}$$

A reduced phase-shift curve $\chi$ may be set up (Fig. 2) with

$$\chi = \beta K_1(\beta) - \tfrac{1}{8}e^{\alpha} 2\beta K_1(2\beta) = -\hbar v B\, \Delta\eta(\beta)/A \quad . \qquad (13)$$

In Fig. 2 the numbers 1, 2, 5, ... within the body of the graph refer to values of $\frac{1}{8}e^{\alpha}$. Until very high velocities, the long-range region of the difference potential controls the monotonic velocity dependence of the cross sections so that, given values for $A$ and $B$, $\bar{Q}$ may be obtained from the graph via Eqs. (10)–(12) by determining the values of $\beta$ versus velocity which correspond to $|\Delta\eta(\beta)|, = 1/\pi$. At high velocities, however, the value of $\alpha$ will become important and a negative deviation from the straight line on the $Q^{1/2}$ versus $\ln v$ will result. The dashed line on Fig. 1 is from such a determination.

The oscillatory portion of the cross sections may now be examined by subtracting $\bar{Q}$. Figure 3 illustrates the plot of $Q_{01} - \bar{Q}$ versus $v^{-1}$. Note the reciprocal velocity dependence of the oscillations and how the envelope of the oscillations increases as the square root of the velocity. Sequencing the oscillations as described before, we make a plot of $N$ versus $v^{-1}$ as shown in Fig. 4. Here, the intercept is $\frac{3}{8}$ (the stationary-phase theoretical intercept) and the slope yields information about $\Delta\eta(b)$ at its maximum (the stationary point). At the maximum, Eq. (5) can be written

$$\Delta\eta(b_0) = -(A/B\hbar v)\chi_{\max} \quad , \qquad (14)$$

where $\chi_{\max}$ is the reduced phase shift $\chi$[Eq. (13)] defined at the maximum. Since the slope equals

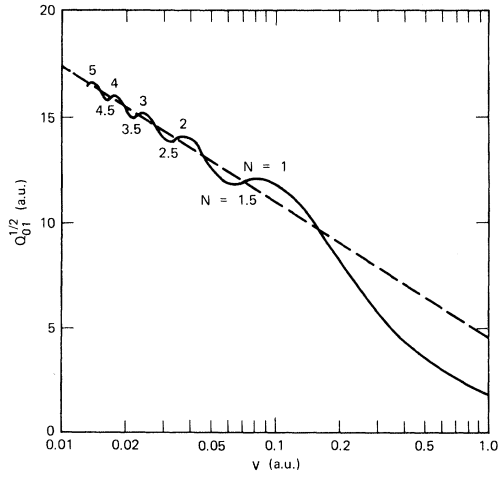


FIG. 1. Resonant total charge-exchange cross sections for the test case $r_e = 5.0$ a.u., $D_e = 0.25$ eV, $\alpha = 2.5$, and $\mu = 843$ a.u. The monotonic dashed line is derived from Eqs. (10)–(12).

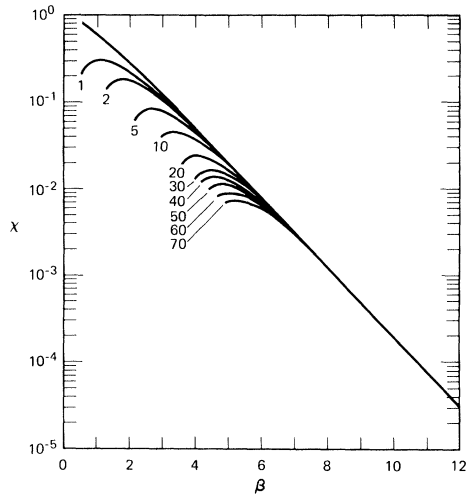


FIG. 2. Plot of $\chi$, as defined by Eq. (13), versus $\beta$ which is equal to $B \cdot b$.

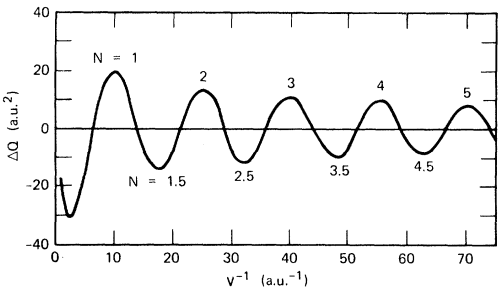


FIG. 3. Plot of $\Delta Q = Q_{01} - \bar{Q}$ versus the reciprocal velocity $v^{-1}$. The cross sections are derived from Fig. 1. The indexing numbers $N$ are included at the extrema.

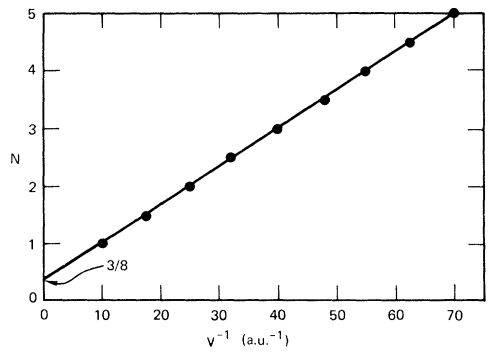


FIG. 4. Illustration of plotting the extrema index number $N$ versus $v^{-1}$ for the test case. Note the $\frac{3}{8}$ intercept. This same intercept may also be obtained by properly indexing the extrema of Ref. 4.

$-\Delta\eta(b_0)/\pi$, we have

$$\pi \times \text{slope} = (A/B\hbar)\chi_{\max} \ ; \tag{15}$$

at the stationary point, $\chi_{\max}$ is governed by $\alpha$. The relationship between $\chi_{\max}$ and $\alpha$ may be seen in Fig. 5.

Until very high velocities, the parameter $\alpha$ does not affect the monotonic portion of the cross sections. Thus the monotonic velocity dependence of the cross sections is determined by the long-range region of the difference potential [Eq. (9)] through the parameters $A$ and $B$. The oscillatory structure yields information about $\alpha$ which, along with $A$ and $B$, specifies the maximum of the difference potential.

The envelopes of the oscillations on Fig. 3 must also be discussed. The envelopes are obtained from the coefficient of the cosine function in Eq. (3). For a difference potential of the form in Eq. (9), we have

$$\frac{d^2\Delta\eta(b_0)}{db^2} = -(AB/\hbar v)[\chi_{\max} - \tfrac{3}{8}e^{\alpha} \times 2\beta_0 K_1(2\beta_0)] \ , \tag{16}$$

in which $\beta_0$ (and hence $b_0$) is defined by

$$K_0(\beta_0) = \tfrac{1}{2}e^{\alpha}K_0(2\beta_0) \ . \tag{17}$$

If we substitute in the potential parameters for this test case, the envelope is equal to $64v^{1/2}$, as confirmed by the calculations.

Furthermore, the often-used relationship[10]

$$\bar{Q}^{1/2} = a - b \ln v \tag{18}$$

is borne out by the linearity of $\log \chi$ versus $\beta$ for large $\beta$ (Fig. 2).

## ANALYSIS OF DATA

The analysis of the experimental data of Perel, Vernon, and Daley proceeds with the use of the graphs presented in the previous section. The square roots of the cross sections are plotted versus $\log v$, and a monotonic cross-section curve is drawn through the data. Since, as we saw in the last section, we have

$$1/\pi = \left|(A/B\hbar v)[\beta_F K_1(\beta_F) - \tfrac{1}{8}e^{\alpha}2\beta_F K_1(2\beta_F)]\right|, \tag{19}$$

and

$$\bar{Q}^{1/2}B^{-1} = \bar{Q}_*^{1/2} = (\tfrac{1}{2\pi})^{1/2}\beta_F \ , \tag{20}$$

the plot of $\chi$ versus $\beta$ may be used to determine the ratio $A/B$ and the quantity $B$.

If at several velocities the square roots of the cross sections are compared to one another, only one segment of the $\chi$ versus $\beta$ plot will satisfy both

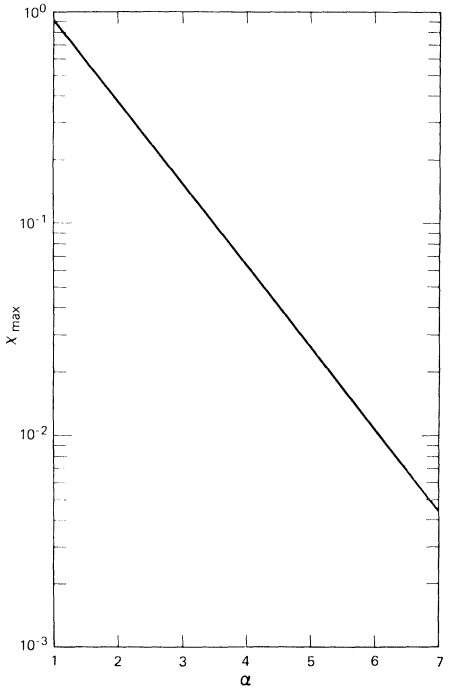


FIG. 5. Graph of $\chi_{\max}$ versus the potential parameter $\alpha$. $\chi_{\max}$ is equal to $\chi$ at its stationary point.

$\chi = \hbar v B/\pi A$ and $\beta_F = (2/\pi)^{1/2}B\bar{Q}^{1/2}$, for constant values of $A$ and $B$. Knowledge of the magnitude of $\bar{Q}^{1/2}$ at some velocity and of its velocity dependence therefore specifies $A$ and $B$, the parameters for the long-range region of the difference potential.

If $N$ versus $v^{-1}$ is plotted, the slope will yield $\alpha$ from Fig. 5 and Eq. (15), since the ratio $A/B$ is known. The various components of $A$ and $B$ (namely, $r_e$, $D_e$, and $\alpha$) may now be deduced.

### $Rb^+$-Rb

The experimental charge-exchange total cross sections of Perel, Vernon, and Daley[2] were used in this analysis. The solid circles of the upper portion of Fig. 6 are a presentation of the data. The straight line drawn through the data is intended to be the monotonic portion of the cross sections. (It is fitted through the high-velocity data, primarily since they have the highest precision. At low velocities, however, the line is within the error bars.) From the plot of $\chi$ versus $\beta$ (Fig. 2) the values of $A/B$ and $B$ are determined to be 4.90 and 0.379.

A plot of $N$ versus $v^{-1}$ is constructed in Fig. 7 from the published values of the maxima given in Ref. 2 and this author's estimates of the minima. There is a slight energy-dependence behavior to

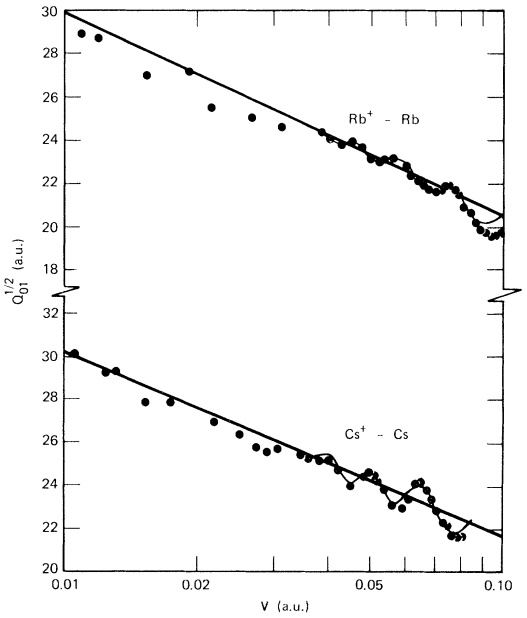


FIG. 6. Upper graph: The square root of the experimental, solid circles, $Rb^+$-Rb cross sections of Perel, Vernon, and Daley versus a logarithmic plot of $v$. Lower graph: The square root of the experimental $Cs^+$-Cs cross sections of the same workers, solid circles, versus a logarithmic plot of $v$. The straight line in both cases is the monotonic portion of the cross section, and the oscillatory one the final fit with the potential parameters of Table I.

the plot. Therefore, if $(N-\frac{3}{8})v$ is plotted versus $v^{-2}$, the zero intercept will yield the value for the slope[11] to be used in the evaluation of $\chi_{max}$ and hence $\alpha$. This energy dependence may be attributed to a slight drift in the experimental measurements[12] or to the fact that Eq. (2) is a high-velocity approximation to the WKB phase shifts. As in low-energy atom-atom scattering, the next order correction will be $-\mathcal{O}v^{-3}$. On the upper portion of Fig. 7 the deviation from the straight-line slope is found to be $E^{-1}$-dependent. The slope of $N$ versus $v^{-1}$ is found to be equal to 0.285, and, with the values of $A$ and $B$, we have $\chi_{max}=0.183$ and $\alpha=2.82$. The equilibrium distance for the ground state is $r_e=7.45$ a.u., and its dissociation energy is $D_e=0.75$ eV. The stationary-point impact parameter is found via Eq. (17) to be $b_0=4.8$ a.u. Nothing can be surmised about the potentials for $r<b_0$. In Fig. 8 the two potentials are presented. It must be pointed out that the quantity determined from the experimental data is the difference potential, and, since Eqs. (7) represent crude separations, the values of $D_e$ and $r_e$ are only qualitative. For the difference potential we find that $R_{max}=5.62$ a.u., and $\Delta V_{max}=3.01$ eV. The potential parameters obtained are summarized in Table I.

A final fit to the data is also illustrated by the curved line in Fig. 6. The magnitude and the positions of the extrema were evaluated by Eqs. (16) and (3).

### $Cs^+$-Cs

As in the $Rb^+$-Rb system, the data of Perel, Vernon, and Daley[2] were used in this analysis. These measurements, along with the monotonic portion of the cross sections, are illustrated in the lower portion of Fig. 6. The derived parameters were $A/B=4.90$ and $B=0.361$. With the slope from the $N$-versus-$v^{-1}$ plot (Fig. 9) equal to 0.237, we have $\chi_{max}=0.152$ and $\alpha=3.03$. The quantities $r_e$ and $D_e$ were found equal to 8.39 a.u. and 0.58 eV, respectively. The same cautionary remarks about $r_e$ and $D_e$ apply as above. Table I lists the various parameters, and Fig. 10 illustrates the two potentials.

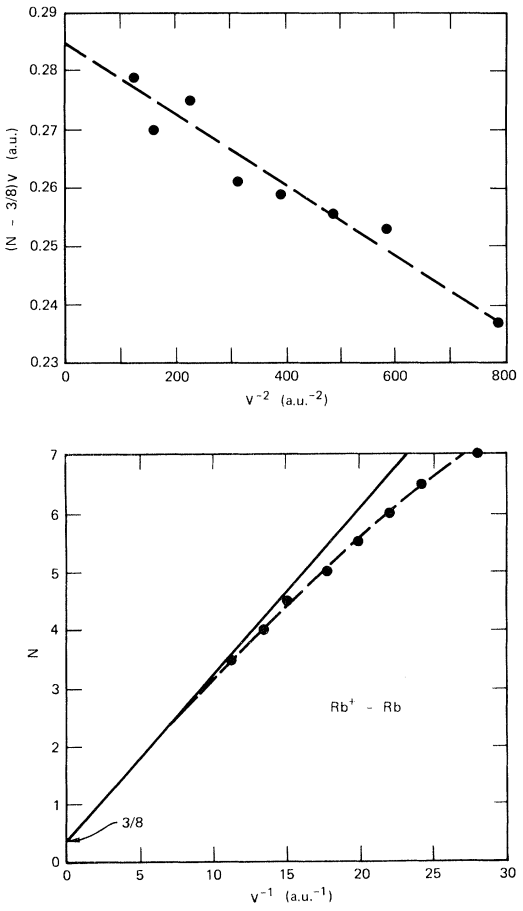


FIG. 7. Lower graph: Plot of $N$ versus $v^{-1}$ for $Rb^+$-Rb, yielding a slope = 0.285. Upper graph: $(N-\frac{3}{8})v$ versus $v^{-2}$, yielding an intercept equal to 0.285 with an $E^{-1}$ dieoff.

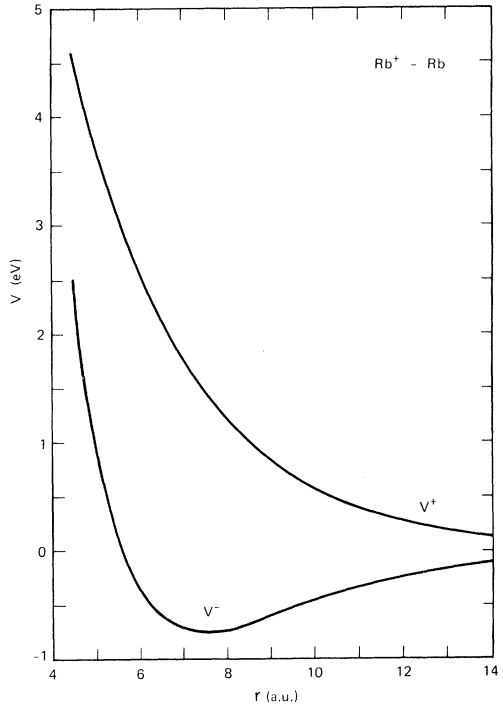


FIG. 8. The internuclear potentials derived from the $Rb^+$-Rb experimental data. The potential parameters are summarized in Table I.

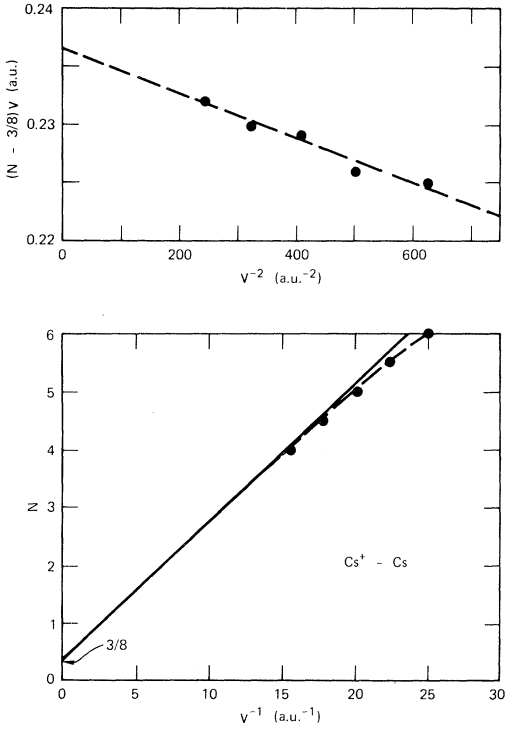


FIG. 9. On the lower graph, $N$ versus $v^{-1}$ for $Cs^+$-Cs is plotted yielding a slope of 0.237. On the upper graph, $(N-\frac{3}{8})\ v$ versus $v^{-2}$ is plotted showing an intercept equal to the 0.237 slope and an $E^{-1}$ decline.

The difference potential peaks at a slightly larger value of internuclear distance than in the Rb case, with $R_{max} = 6.47$ a.u. and $\Delta V_{max} = 2.32$ eV. The product $R_{max} \times \Delta V_{max}$ is less in the Cs system than in the Rb system, as is the slope of the $N$-versus-$v^{-1}$ plot. In general, from a logical ex-

TABLE I. Derived potential constants.

| | $Rb^+$-Rb | $Cs^+$-Cs This analysis | Smith[a] |
|---|---|---|---|
| $R_{max}$ (a.u.) | 5.62 | 6.47 | 7.0 |
| $\Delta V_{max}$ (eV) | 3.01 | 2.32 | 2.0 |
| $r_e$ (a.u.) | 7.45 | 8.39 | 10.1 |
| $D_e$ (eV) | 0.75 | 0.58 | 0.50 |
| $\alpha$ | 2.82 | 3.03 | 3.92 |
| $\beta$[b] | 0.379 | 0.361 | 0.388 |

[a]Reference 3.

[b]This is the $\beta$ spectroscopic parameter of G. Herzberg, Spectra of Diatomic Molecules (D. Van Nostrand, Inc., New York, 1950), 2nd ed., p. 101. Please do not confuse it with the reduced impact parameter used in the text.

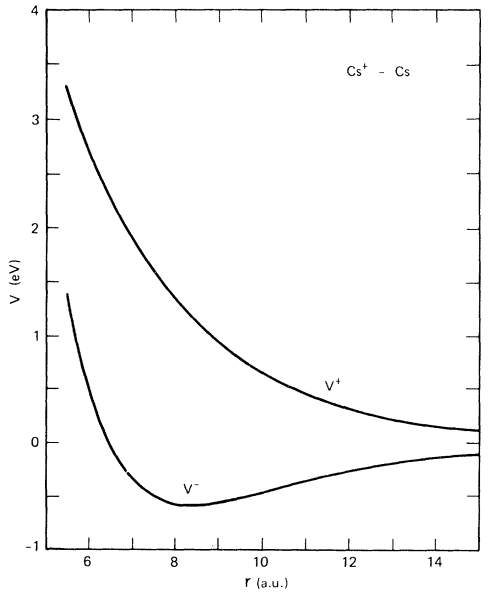


FIG. 10. The final internuclear potentials obtained from the $Cs^+$-Cs experimental data. The potential parameters are summarized in Table I.

tension of the atom-atom glory oscillations, and from Eq. (14), it may be stated that, assuming a constant curvature of the difference potential (in this case, constant $\alpha$) at the maximum, the slope will be roughly proportional to the $R_{max} \times \Delta V_{max}$ product.[11,13]

The final fit to the data is shown in Fig. 6. As before, the magnitude and positions of the extrema were evaluated via Eqs. (16) and (3).

### CHECK CASE: $Li^+$-Li

The theoretical calculations[4] on $Li^+$-Li provide a check not only on the method but also on the error limits to be expected for the functionality used in the difference potential, Eq. (9). The calculations on the resonant charge-exchange total cross sections were by formulas different from Eqs. (1) and (2), and utilized the *ab initio* potential computations of Michels.[14] On Fig. 11 the oscillatory line is the result of these calculations. The dashed line is the experimental results of Lorents, Black, and Heinz.[15]

A straight line is plotted through the oscillations, and the parameters $A$ and $B$ are determined as in the previous section. The values obtained are $A = 3.02$ and $B = 0.474$. From the plot of the indexing numbers for the extrema versus the reciprocal velocity (Fig. 12) $\alpha$ is found equal to 2.85. It should be noted that the $\frac{3}{8}$ intercept is obtained.

Figure 13 illustrates the retrieved difference

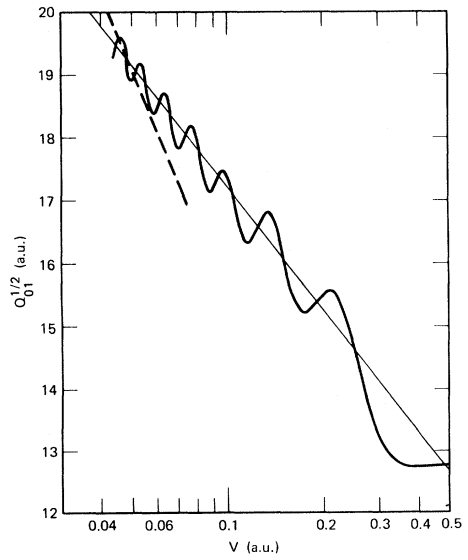


FIG. 11. The oscillatory line represents the theoretical calculations of Peek, Green, Perel, and Michels (Ref. 4) on the $Li^+$-Li system. The dashed line is the experimental values of Lorents, Black, and Heinz (Ref. 15).

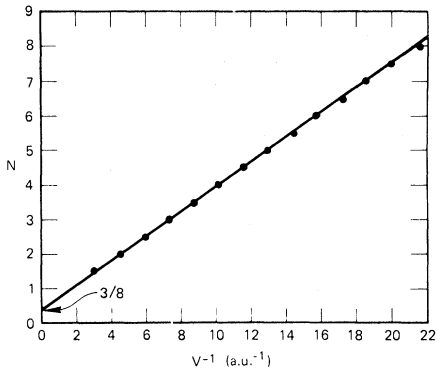


FIG. 12. The indexing number $N$ is plotted versus the reciprocal velocity for the oscillations presented in Fig. 11.

potential with that used in the calculation. The value of $R_{max} = 4.55$ a.u. is 9% low, and the value of $\Delta V_{max} = 0.175$ a.u., is 20% low. However, the curvature of the retrieved difference potential is greater than that of Michels.

The stationary-point impact parameter was found equal to 3.9 a.u. so that no comparison can be made for $r$ less than this value. If the separation is made to the potentials given by Eqs. (7), we have the parameter $D_e = 0.044$ a.u., and the parameter $r_e = 6.01$ a.u.

As can be seen by Eq. (14), the frequency of the oscillations will be governed by the difference potential in the form $A\chi_{max}/B$, which is proportional to the product $\Delta V_{max} \times R_{max} \times a(\kappa)$, where $a(\kappa)$ is a parameter determined by the reduced curvature $\kappa$ at the difference potential maximum.[16]

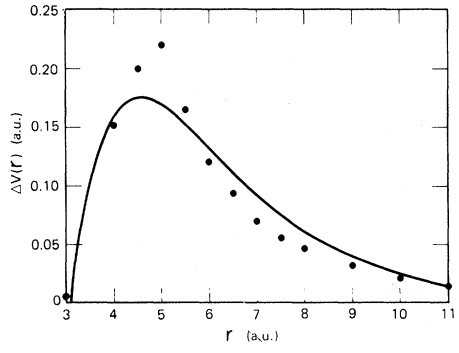


FIG. 13. The difference potential (solid line) which was retrieved from the theoretical charge-exchange total cross sections (Ref. 4) via the methods in the text is shown along with the potential energy differences of Michels (Ref. 14) from which the cross sections were calculated.

As the difference potential maximum becomes broader, $a(\kappa)$ increases and vice versa. This allows a complete family of curves to fit the oscillations. The only other constraint is that the long-range portion of the difference potential must fit the monotonic velocity dependence of the cross sections.

In this case, the derived difference potential will fit the monotonic velocity dependence and the frequency of the oscillations of the cross sections. The only observable left is the amplitude of the oscillations. With the parameters from the retrieved difference potential and Eqs. (3) and (16), the envelope of the oscillations is found to be $40.9\ v^{1/2}$. This agrees almost perfectly with the calculations.

Since the cross sections contain three, and maybe four, bits of information, it is unrealistic to assume that a unique potential can be obtained from them without more information. However, it is reasonable to assume that a flexibly parametrized form for the difference potential, containing no more parameters than the amount of information, should return a difference potential which agrees to within about 25% with the "true" difference potential.

## SUMMARY AND CONCLUSIONS

A systematic procedure for analyzing the resonant total charge-exchange cross sections has been set up to obtain the difference potential responsible for the scattering. The monotonic velocity-dependent portions of the experimental cross sections are employed to obtain information about the long-range forces. These are combined with information obtained about the maximum in the difference potential from the oscillatory structure of the cross sections to generate a difference potential over a large range of internuclear separations.

Two systems were analyzed, those of $Rb^+$-Rb and $Cs^+$-Cs. It was found that the difference potential in the Rb system maximized at 5.62 a.u. with a magnitude of 3.01 eV. The bowl of the low-lying state was found to be characterized by $r_e = 7.45$ a.u. and $D_e = 0.75$ eV. These last two parameters are, of course, dependent upon a correct separation of the difference potential into its two states. Nor information, however, can be implied about either potential for $r \lesssim 4.8$ a.u.

In the Cs system the maximum occurred at a slightly greater internuclear separation, $R_{max} = 6.47$ a.u., but with a smaller magnitude, $\Delta V_{max} = 2.32$ eV. The bowl of the low-lying state could be parametrized by $r_e = 8.39$ a.u. and $D_e = 0.58$ eV. The experimental data did not yield any information about the potentials for $r \lesssim 5.6$ a.u. The potential parameters are in fair agreement with those of Smith,[3] who previously analyzed this system and found $r_e = 10.1$ a.u., $D_e = 0.50$ eV, $R_{max} = 7.0$ a.u., and $\Delta V_{max} = 2.0$ eV.

In comparing the slopes of the $N$-versus-$v^{-1}$ plots for the two systems, it is noted that the slope for Rb is greater than that of the Cs system. A further increase is indicated by the work[4] on $Li^+$-Li. If there is a correspondence relationship for the alkalis, it would be expected that the slopes will be in the following order: Li > Na > K > Rb > Cs. (Preliminary experimental measurements on the Li and Na systems confirm this trend.[17]) Such a relationship implies that, assuming constant curvature at the difference potential maximum, the product $R_{max} \times \Delta V_{max}$ will follow the same order. Since $R_{max}$ varies slightly, the magnitude of $\Delta V_{max}$ will also follow the above order. This is in agreement with an estimate (due to Peek *et al.*[4]) of the difference potential for $Li^+$-Li in which $R_{max} \cong 5.0$ a.u. and $\Delta V_{max} \cong 6.0$ eV.

Several cautionary remarks should be made concerning the uniqueness of the difference potential obtained from the experimental cross sections. Since the measurements indicate that they follow the relationships

$$Q = \overline{Q} - cv^{1/2}\cos(dv^{-1} + \tfrac{1}{4}\pi) \ ,$$

where $\overline{Q} = (a - b\ln v)^2$ ,

only four parameters ($a, b, c$, and $d$) are necessary to parametrize the velocity dependence of the cross sections; hence four bits of information are contained within them. Since the parameter $c$ is generally insensitive to reasonable changes in the difference potential maximum (as is seen in the $Li^+$-Li comparison) only three parameters may be justified until much more accurate data is obtained. Within these three, the parameter $d$ yields information about the difference potential maximum only in the form of the product $\Delta V_{max} \times R_{max} \times a(\kappa)$, where $a(\kappa)$ is a factor related to the curvature at the maximum. With this uncertainty added to the possibility of an incorrect parametrization of the difference potential [Eq. (9)], this author would estimate possible errors in the difference potential to be about ±25%. The separated potentials [Eqs. (7) and Figs. 8 and 10] are obtained from a separation justified only at large internuclear distances; hence the "true" potentials may be far removed from those given, particularly for $r < r_e$. These potentials do, however, make it possible to give a first estimate for such scattering phenomena as the differential and total cross sections. The above uncertainties can be reduced somewhat only when independent measurements, such as differential scattering, or accurate *ab initio* potential calculations, as in the $Li^+$-Li case, become available.

## ACKNOWLEDGMENT

The author would like to thank Dr. Julius Perel for many valuable suggestions.

*The author wishes to thank the Atholl McBean Foundation of the Stanford Research Institute for funding this research.

[1]D. R. Bates and R. McCarroll, Advan. Phys. 11, 39 (1962).
[2]J. Perel, R. H. Vernon, and H. L. Daley, Phys. Rev. 138, A937 (1965).
[3]F. J. Smith, Phys. Letters 20, 271 (1966).
[4]J. M. Peek, T. A. Green, J. Perel, and H. H. Michels, Phys. Rev. Letters 20, 1419 (1968).
[5]K. W. Ford and J. A. Wheeler, Ann. Phys. (N. Y.) 7, 259 (1959).
[6]O. Firsov, Zh. Eksperim. i Teor. Fiz. 21, 1001 (1951).
[7]R. B. Bernstein, J. Chem. Phys. 38, 2599 (1963); R. Düren and H. Pauly, Z. Physik 175, 227 (1963); 177, 146 (1964).
[8]These are the same potential forms that were used by E. A. Mason and J. T. Vanderslice, J. Chem. Phys. 29, 361 (1958).
[9]T. J. M. Boyd and A. Dalgarno, Proc. Phys. Soc. (London) 72, 694 (1958).
[10]A. Dalgarno, Phil. Trans. Roy. Soc. London A250, 426 (1958); D. Rapp and W. E. Francis, J. Chem. Phys. 37, 2631 (1962).
[11]R. B. Bernstein and T. J. P. O'Brien, Discussions Faraday Soc. 40, 35 (1965); R. B. Bernstein and T. J. P. O'Brien, J. Chem. Phys. 46, 1208 (1967).
[12]From recent measurements Dr. Perel now believes this is the case (private communication).
[13]R. E. Olson, J. Chem. Phys. 50, 554 (1969).
[14]H. H. Michels (unpublished).
[15]D. C. Lorents, G. Black, and O. Heinz, Phys. Rev. 137, A1049 (1965).
[16]The reduced curvature is the second derivative of the reduced $\Delta V(r)$, with respect to $r$ at $r$ equal to unity. The reduced $\Delta V(r)$ has $R_{max}=\Delta V_{max}=1.0$.
[17]J. Perel (private communication).

PHYSICAL REVIEW VOLUME 187, NUMBER 1 5 NOVEMBER 1969

# Charge-Transfer Cross Sections for $H^+$, $Li^+$, and $Na^+$ on $N_2$ †

Grant J. Lockwood
*Sandia Laboratories, Albuquerque, New Mexico* 87115
(Received 26 May 1969)

Measurements of the total cross section for charge transfer $\sigma_{10}$ of $H^+$, $Li^+$, and $Na^+$ on $N_2$ are reported here in the energy range of 25–100 keV. The method used was direct detection of fast neutral particles that were formed in single charge-transfer collisions. Data for $H^+$ on $N_2$ are in excellent agreement with previously published results with $\sigma_{10}$ increasing with decreasing energy, reaching a value of $1.55\times10^{-15}$ cm$^2$/molecule at 5 keV. From data for $Li^+$ and $Na^+$ on $N_2$, $\sigma_{10}$ is observed to increase with increasing energy. The cross section for $Na^+$ has a maximum of $1.1\times10^{-16}$ cm$^2$/molecule at about 50 keV, while the cross section for $Li^+$ is still increasing at 100 keV, although an irregularity is observed at approximately 30 keV.

## I. INTRODUCTION

Measurements have been reported of the total cross sections for charge transfer of $Li^+$ and $Na^+$ on $N_2$ by Ogurtsov *et al.*[1] in the energy range ~1–30 keV by detecting the fast neutral particles formed in single charge-transfer collisions. This method has been used in the present study which extends the energy range to 100 keV. In addition, the charge-transfer cross section for $H^+$ on $N_2$ by this method is included. This result is compared with data reported by other investigators[2–4] using other techniques.

The method's main shortcoming is that neutrals scattered through an angle larger than 1° are not detected. This can cause the value of the cross section to be low at low energy, but in the energy range covered here this does not appear to be the case. Jones *et al.*[5] have measured the contribution to the total cross section for particles scattered between 0° and 1°. For charge transfer of noble-gas ions in noble gases, at 25 keV all cases showed that 96% or more of the total cross section was contained between 0° and 1°, with the exception of $Ne^+$ on Ar where only 85% was measured between 0° and 1°.

Section II describes the apparatus and procedure used to obtain the data. Data are presented and discussed in Sec. III, and comparisons are made with data of other investigators.[3,6]